Online Appendix to

Asset Diversification versus Climate Action

Christoph Hambel[1] Holger Kraft[2] Frederick van der Ploeg[3]

Revised version: November 2023

Abstract:

Here we present additional material such as the description of the solution approach, analysis of the policy functions, the simulation results, and additional robustness checks.

[1] Tilburg University, Department of Econometrics and Operations Research
E-mail: C.Hambel@tilburguniversity.edu

[2] Faculty of Economics and Business, Goethe University, Theodor-W.-Adorno-Platz 3, 60323 Frankfurt am Main, Germany. Phone: +49 (0) 69 798 33699.
E-mail: holgerkraft@finance.uni-frankfurt.de

[3] University of Oxford, Department of Economics, OXCARRE, Manor Road Building, Oxford OX1 3UQ, U.K. Phone: +44 (0) 1865 281285.
E-mail: rick.vanderploeg@economics.ox.ac.uk. Also affiliated with ASE, University of Amsterdam, P.O. Box 15551, 1001 NB Amsterdam, the Netherlands, and CEPR.

Table of Contents

B Numerical Solution Approach

B.1 Value Function and Optimal Controls

Basic idea We face a problem with an infinite time horizon. To solve this problem we first compute the steady state $\widetilde{G}(T,S)$ on a two-dimensional grid (T,S) assuming there is no exogenous time trend. Thus we first have to solve a similar PDE as in (A.10) but without the time derivative. The resulting steady state $\widetilde{G}(T,S)$ is then used as a terminal condition $G(t_{\max},T,S) = \widetilde{G}(T,S)$ for the value function in the year 2620 corresponding to $t_{\max} = 600$. Starting with this terminal condition, we proceed backwards through the time grid to analyze the transition towards the steady state.

Definition of the grid We use a grid-based solution approach to solve the non-linear PDE. We discretize the (t,T,S)-space using an equally-spaced lattice. Its grid points are defined by

$$\big\{(t_n,T_i,S_j) \mid n = 0,\cdots,N_t,\, i = 0,\cdots,N_T,\, j = 0,\cdots,N_S\big\},$$

where $t_n = n\Delta_t$, $T_i = i\Delta_T$, and $S_j = j\Delta_S$ for some fixed grid size parameters Δ_t, Δ_T, and Δ_S that denote the distances between two grid points. The numerical results are based on a choice of $N_T = 50$, $N_S = 300$ and 1 time step per year. Our results hardly change if we use a finer grid or more time steps per year. In the sequel, $G_{n,i,j}$ denotes the approximated value function at the grid point (t_n,T_i,S_j) and $\pi_{n,i,j}$ refers to the corresponding set of optimal controls. We apply an implicit finite-difference scheme.

Finite differences approach In this paragraph, we describe the numerical solution approach in more detail. We adapt the numerical solution approach used by Munk and Sørensen (2010). The numerical procedure works as follows. At any point in time, we make a conjecture for the optimal strategy $\pi^*_{n,i,j}$. A good guess is the value at the previous grid point since the abatement strategy varies only slightly over a small time interval, i.e., we set $\pi_{n-1,i,j} = \pi^*_{n,i,j}$. Substituting this guess into the HJB equation yields a semi-linear PDE:

$$0 = \delta\theta G^{1-1/\theta} c^{1-1/\psi} + M_1 G + M_2 G_T + M_3 G_{TT} + M_4 G_S + M_5 G_{SS}$$

with state-dependent coefficients $M_i = M_i(t,T,S)$ as stated in Appendix A.1. Due to the implicit approach, we approximate the time derivative by forward finite differences. In the approximation, we use the so-called 'up-wind' scheme that stabilizes the finite differences approach. Therefore, the relevant finite differences at the grid point (n,i,j) are given by

$$\begin{aligned}
&\mathrm{D}_T^+ G_{n,i,j} = \frac{G_{n,i+1,j} - G_{n,i,j}}{\Delta_T}, \qquad \mathrm{D}_T^- G_{n,i,j} = \frac{G_{n,i,j} - G_{n,i-1,j}}{\Delta_T},\\
&\mathrm{D}_S^+ G_{n,i,j} = \frac{G_{n,i,j+1} - G_{n,i,j}}{\Delta_S}, \qquad \mathrm{D}_S^- G_{n,i,j} = \frac{G_{n,i,j} - G_{n,i,j-1}}{\Delta_S},\\
&\mathrm{D}_{TT}^2 G_{n,i,j} = \frac{G_{n,i+1,j} - 2G_{n,i,j} + G_{n,i-1,j}}{\Delta_T^2}, \qquad \mathrm{D}_{SS}^2 G_{n,i,j} = \frac{G_{n,i,j+1} - 2G_{n,i,j} + G_{n,i,j-1}}{\Delta_S^2},\\
&\mathrm{D}_t^+ G_{n,i,j} = \frac{G_{n+1,i,j} - G_{n,i,j}}{\Delta_t}.
\end{aligned}$$

Substituting these expressions into the PDE above yields the following semi-linear equation for the grid point (t_n, m_i, τ_j):

$$\begin{aligned}
G_{n+1,i,j}\frac{1}{\Delta_t} = G_{n,i,j}\Big[&- M_1 + \frac{1}{\Delta_t} + \mathrm{abs}\Big(\frac{M_2}{\Delta_T}\Big) + \mathrm{abs}\Big(\frac{M_4}{\Delta_S}\Big) + 2\frac{M_3}{\Delta_T^2} + 2\frac{M_5}{\Delta_S^2}\Big]\\
&+ G_{n,i-1,j}\Big[\frac{M_2^-}{\Delta_T} - \frac{M_3}{\Delta_T^2}\Big] + G_{n,i+1,j}\Big[-\frac{M_2^+}{\Delta_T} - \frac{M_3}{\Delta_T^2}\Big]\\
&+ G_{n,i,j-1}\Big[\frac{M_4^-}{\Delta_S} - \frac{M_5}{\Delta_S^2}\Big] + G_{n,i,j+1}\Big[-\frac{M_4^+}{\Delta_S} - \frac{M_5}{\Delta_S^2}\Big]\\
&+ \delta\theta G_{n,i,j}^{1-1/\theta} c_{n,i,j}^{1-1/\psi}.
\end{aligned}$$

Therefore, for a fixed point in time each grid point is determined by a non-linear equation. This results in a non-linear system of $(N_S+1)(N_T+1)$ equations that can be solved for the vector

$$G_n = (G_{n,1,1}, \cdots, G_{n,1,N_S}, G_{n,2,1}, \cdots, G_{n,2,N_S}, \cdots, G_{n,N_T,1}, \cdots, G_{n,N_T,N_S}).$$

Using this solution we update our conjecture for the optimal controls at the current point in the time dimension. We apply the first-order conditions and the above mentioned finite difference approximations of the corresponding derivatives.

B.2 Stochastic Discount Factor and Risk Premia

The dynamics of the SDF and the asset prices involve some yet unknown variables. For instance, the risk-free rate (7.1) involves the unknown drift and volatility vector of the consumption-capital ratio. These variables depend on the reduced-form value function G in (A.3) and its partial derivatives in a highly nonlinear manner. We thus calculate these variables numerically using finite differences. An application of Itôs lemma to $c = c(t,S,T)$ implies

$$\mathrm{d}c = c_t \mathrm{d}t + c_S \mathrm{d}S + c_T \mathrm{d}T + \frac{1}{2} c_{TT} \|\sigma_T\|^2 \mathrm{d}t + \frac{1}{2} c_{SS} \|\sigma_S\|^2 \mathrm{d}t,$$

where

$$\mu_c(t,S,T) = \frac{1}{c}\big[c_t + c_S S(1-S)\mu_S + c_T \mu_T + \frac{1}{2} c_{TT}\|\sigma_T\|^2 + \frac{1}{2} c_{SS} S^2 (1-S)^2 \|\sigma_S\|^2\big], \tag{B.1}$$

$$\sigma_c(t,S,T) = \frac{1}{c}\big[c_S S(1-S)\sigma_S + c_T \sigma_T\big]. \tag{B.2}$$

Since c is given by equation (A.2) and the optimal controls have already been calculated, we can use finite differences again to determine c and its partial derivatives. Then, we substitute them into equations (B.1) and (B.2) to get the relevant drift and volatility vectors.

C State-Space Solutions

Here we discuss the influence of the state variables on the optimal decisions and asset returns. From this, we derive intuition for the influence of the share of brown capital and temperature on the optimal controls and understand the economic forces at play. In particular, we discuss how climate change affects the interest rate and asset returns. All the results are for the benchmark calibration for the year 2100 and for the level impact (L–I) climate damages. The policy functions behave in a qualitatively similar manner for other years and for our alternative parametrizations of damages. The qualitative behavior of the asset returns is hardly affected by the choice of the damage specification.

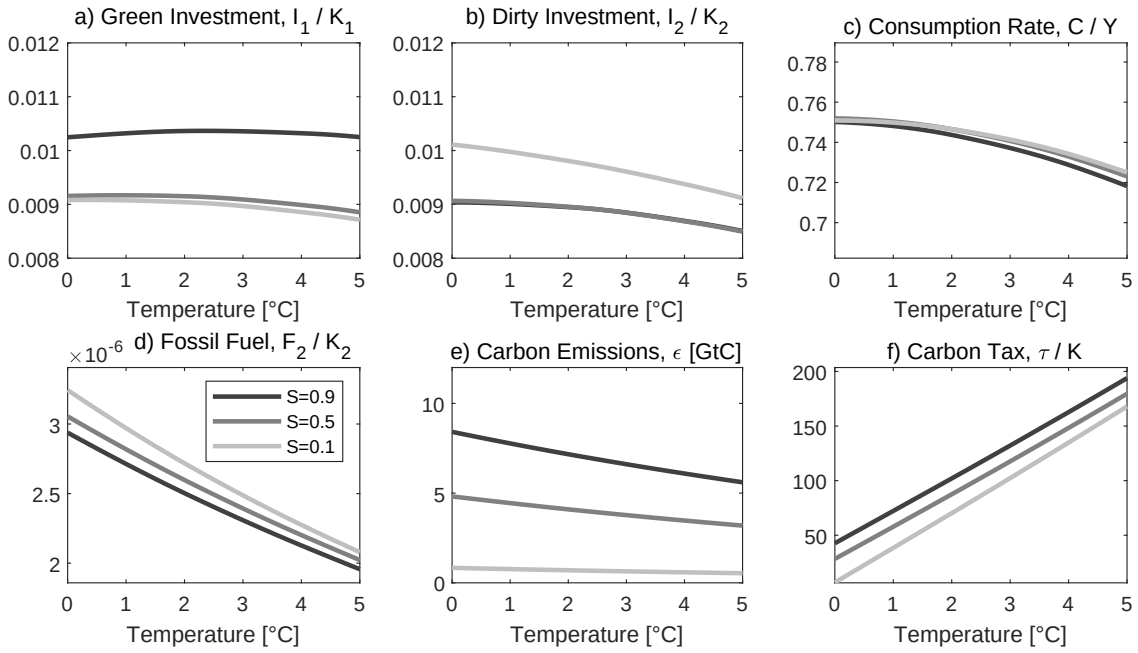

Figure A.1: Policy Functions with Level Impact of Climate Change as function of S and T. The graphs depict policy rules as functions of the two state variables. On the horizontal axis is temperature in the range from 0°C to 5°C. The lines represent various levels of the capital share: dark lines (——) depict $S = 0.9$, gray lines (——) refer to $S = 0.5$, and light (——) lines to $S = 0.1$. a) plots green investment as fraction of green capital, b) shows brown investment as fraction of brown capital, c) depicts consumption as fraction of output, d) shows green energy as fraction of green capital, e) depicts fossil fuel use as fraction of brown capital, and f) shows the optimal carbon tax as fraction of total capital.

C.1 State-Space Effects of Climate Policy on the Economy

The lines in Figure A.1 present various levels of the capital share. The dark lines (——) depict $S = 0.9$, the gray lines (——) refers to $S = 0.5$, and the light lines (——) to $S = 0.1$. The horizontal axis depicts the temperature in the range from 0°C to 5°C.

Panel a) of Figure A.1 shows that the optimal investment in the green capital stock decreases in the share of brown capital S, whereas Panel b) shows that the opposite is true for the investment in the brown capital stock. This can be explained by the diversification argument discussed in Section 3. If damages are moderate (as for the DICE damage specification), the economy retains a certain level of brown capital to reach an optimal level of diversification. Therefore, the agent invests more in the green capital stock if the share of brown capital is high and more in the brown capital stock if this share is low. Panel c) shows that the optimal consumption strategy hardly depends on the share of brown capital. This reflects the agent's motive for consumption smoothing. Instead of adjusting the consump-

tion rate in response to the changes in the share of brown capital, the economy increases the green investment ratio and decreases the brown investment ratio to smooth consumption. Panel d) depicts fossil fuel use relative to the respective capital stock, which does not vary very much with the share of brown capital. The corresponding ratio for green energy, F_1/K_1, does not depend on the share of brown capital at all.[36] Panel e) depicts carbon emissions and shows that in absolute terms fossil fuel use decreases both in the share of brown capital and temperature.

Panel f) depicts the optimal carbon tax as a fraction of total capital. It shows that the optimal carbon tax sharply increases in temperature and increases only moderately in the share of brown assets. In recent years, a literature has evolved that derives simple formulas for the optimal SCC in deterministic environments (e.g., Nordhaus 1991; Golosov et al. 2014, Rezai and van der Ploeg 2016; van den Bijgaart et al. 2016; van der Ploeg and Rezai 2019 and Hambel et al. 2021b). This strand of literature considers analytical models and generates a SCC that does not depend on temperature.[37] By contrast, our framework explicitly models stochastic climate risks and uses a convex damage function, which yields temperature-dependent carbon taxes and optimal controls. Consequently, society reacts to increasing climate risks by raising carbon taxes and thus to more pronounced carbon abatement for higher temperatures. For the climate disaster impact, damages are linear in temperature rather than convex. In turn, the policy functions are almost independent of temperature as in the above mentioned strand of literature.[38]

C.2 State-Space Effects of Climate Policy on Asset Prices

This section provides some additional material on the effect of climate policy on asset prices referred to in the paper. Figure A.2 complements Figure 7 in the main text, but it disregards the option to convert brown capital into green capital. Figure A.3 depicts the asset pricing implications for the disaster impact. Table A.1 provides a static decomposition of the risk-free rate to analyze how the state variables S and T affect its several components.

[36] See the first-order condition (3.4).

[37] The reason is that the concavity of the logarithmic Arrhenius' law linking temperature to the atmospheric stock of carbon is (more or less) exactly offset by the convexity of the function relating the damage ratio to temperature (Golosov et al. 2014). For more convex damage ratios, the ratio of the optimal SCC to GDP increases in temperature (e.g., Rezai and van der Ploeg 2016).

[38] The corresponding figures are available upon request.

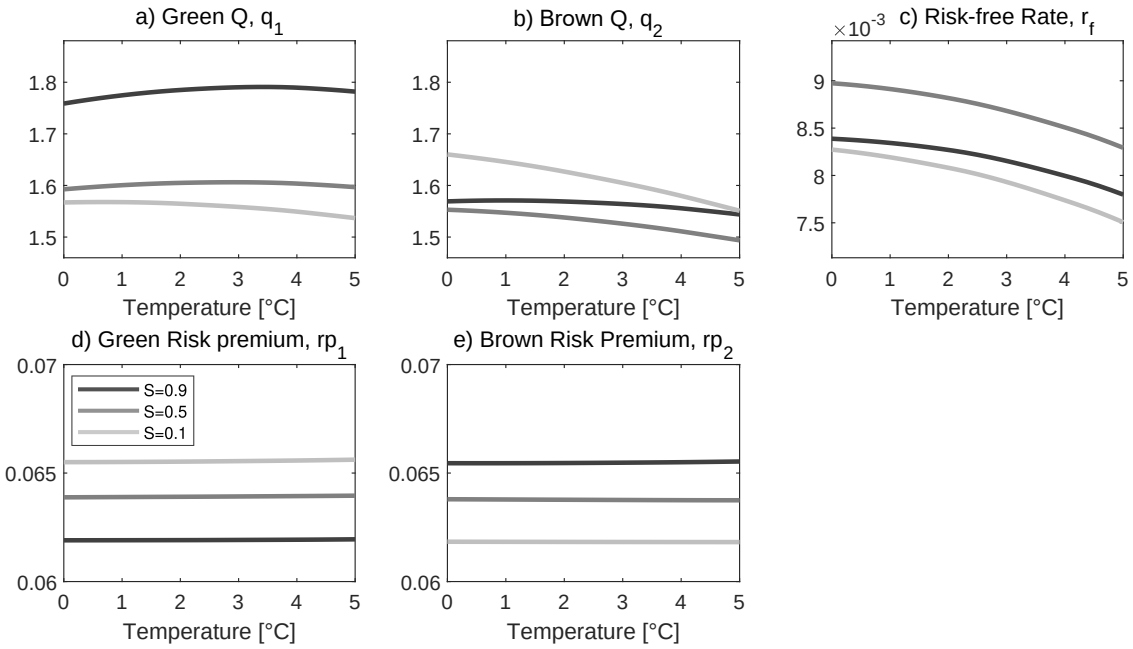

Figure A.2: Asset Pricing without Option to Convert as function of *S* and *T*. This figure complements Figure 7 and depicts the corresponding results if the option to convert is disregarded. On the horizontal axis is temperature in the range from 0°C to 5°C. The lines represent various levels of the capital share: dark lines (——) depict $S = 0.9$, gray lines (——) refer to $S = 0.5$, and light (——) lines to $S = 0.1$. a) plots Tobin's Q of the green asset, b) shows Tobin's Q of the brown capital stock, c) depicts the equilibrium risk-free rate, d) shows the risk premium of the green asset, e) depicts the risk premium of the brown asset.

D Optimal Policy Simulations: Additional Results

Here we present our optimal policy simulation results over the next 100 years. The columns of Figures A.4 and A.5 show results for the two climate damage specifications (L–I), and (D–I), respectively. Unless otherwise stated, we use the benchmark calibration summarized in Table 1. Optimal paths are depicted by solid lines (——) and BAU paths by dotted lines (·····). Dashed lines (- - -) show 5% and 95% quantiles of the optimal solution. Appendix C shows the state-space solutions that are used to get these simulations.

D.1 Effects of Climate Policy on the Economy

Figure A.4 depicts the optimal evolution of the real economy under two different climate damage specifications. It shows that the qualitative behavior is similar for all specifications. Panels a1)-a2) depict the time paths of output. As a result of climate action, the optimal evolutions exhibit a higher economic growth compared to the BAU evolution since some

(a)	r_f	$\frac{1}{\psi}\mu_C$	Diff Risk
$T = 1°C$	0.88%	4.83%	–0.12%
$T = 2°C$	0.87%	4.81%	–0.12%
$T = 3°C$	0.84%	4.78%	–0.12%
$T = 4°C$	0.81%	4.76%	–0.12%
$T = 5°C$	0.77%	4.71%	–0.12%
$S = 0.05$	0.78%	4.79%	–0.19%
$S = 0.25$	0.82%	4.79%	–0.14%
$S = 0.50$	0.84%	4.79%	–0.11%
$S = 0.75$	0.81%	4.78%	–0.14%
$S = 0.95$	0.78%	4.79%	–0.19%

(b)	r_f	$\frac{1}{\psi}\mu_C$	Diff Risk	Climate Disaster
$T = 1°C$	0.57%	4.88%	–0.21%	-0.27%
$T = 2°C$	0.36%	4.92%	–0.21%	-0.53%
$T = 3°C$	0.14%	4.96%	–0.21%	-0.79%
$T = 4°C$	–0.07%	5.01%	–0.21%	-1.05%
$T = 5°C$	–0.29%	5.05%	–0.21%	-1.31%
$S = 0.05$	0.43%	4.91%	–0.19%	-0.46%
$S = 0.25$	0.47%	4.91%	–0.14%	-0.46%
$S = 0.50$	0.49%	4.90%	–0.11%	-0.46%
$S = 0.75$	0.43%	4.86%	–0.14%	-0.46%
$S = 0.95$	0.34%	4.82%	–0.19%	-0.46%

Table A.1: Decomposition of the Risk-free Rate for the Year 2100. The table shows the state-dependent terms in the decomposition of the risk-free rate (7.1) for the Nordhaus level damage specification (a) and the climate disaster impact (b). It provides sensitivity analysis for different values of temperature and the share of brown capital around their median values in 2100 ($S = 0.44$, $T = 2.9°C$ for the Nordhaus damages and ($S = 0.05$, $T = 1.8°C$ for climate disasters). The constant terms in (7.1) are the time preference rate $\delta = 0.015$, and the contribution of economic disasters $\lambda_e \mathbb{E}[(1-\ell_e)^{-\gamma} - 1 - \frac{\psi^{-1}-\gamma}{1-\gamma}(1-(1-\ell_e)^{1-\gamma})] = -0.0533$. The temperature interaction terms corresponding to the last line in (7.1) are close to zero and do not significantly contribute to the equilibrium interest rate. A similar table for the disaster impact is available upon request.

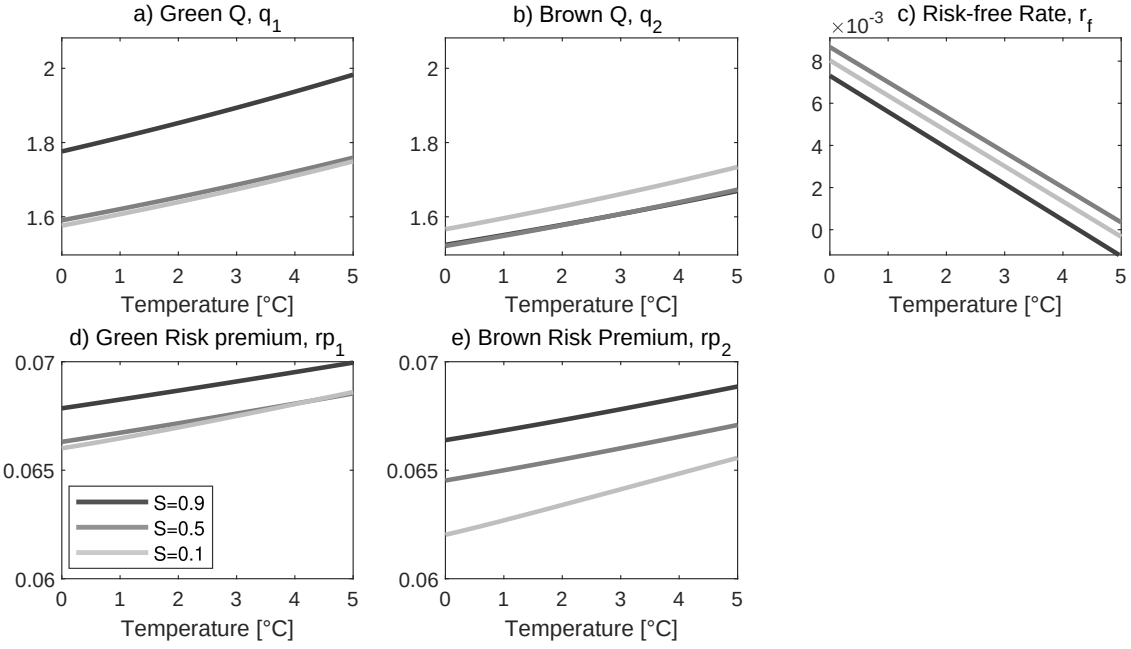

Figure A.3: Asset Pricing versus Temperature and the Share of Brown Capital (Climate Disasters). On the horizontal axis is temperature in the range from 0°C to 5°C. The lines represent various levels of the capital share: dark lines (——) depict $S = 0.9$, gray lines (——) refer to $S = 0.5$, and light (——) lines to $S = 0.1$. a) plots Tobin's Q of the green asset, b) shows Tobin's Q of the brown capital stock, c) depicts the equilibrium risk-free rate, d) shows the risk premium of the green asset, e) depicts the risk premium of the brown asset. The option to convert brown into green capital generates interesting qualitative effects but the quantitative implications are moderate.

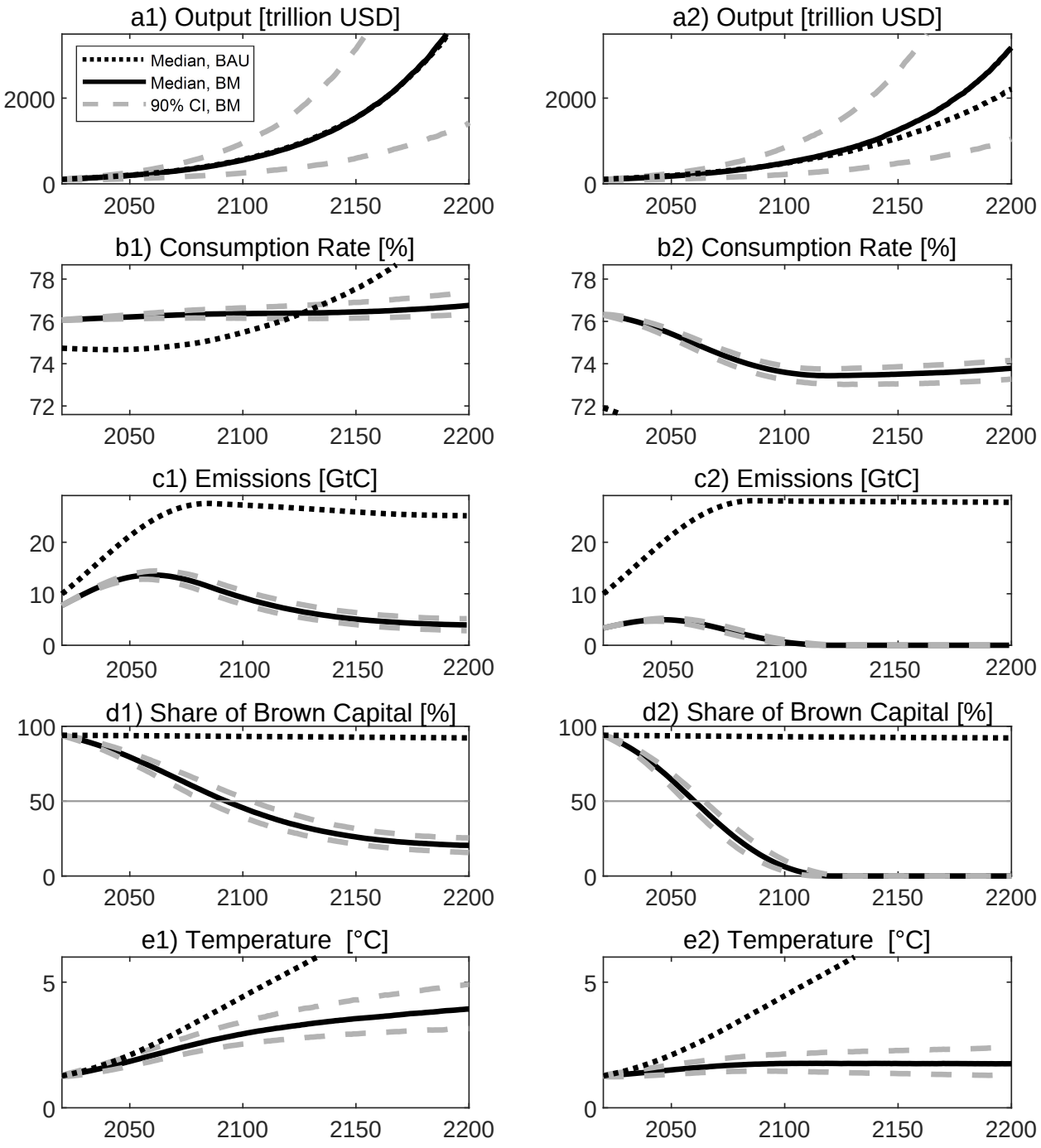

Figure A.4: Evolution of Temperature, the Social Cost of Carbon and the Real Economy. The figure depicts the simulation of the real economy for the two climate damage specifications level impact (1st column) and disaster impact (2nd column) until the year 2200. Median optimal paths are depicted by solid lines (——) and median BAU paths by dotted lines (·····). Dashed lines (- - -) show 5% and 95% quantiles of the optimal solution. Panels a1)-a2) show the evolution of output. Panels b1)-b2) depict the consumption rate expressed as a fraction of output, i.e., C/Y. Panels c1)-c2) depict the evolution of carbon emissions. Panels d1)-d2) show the evolution of the share of brown capital S. Panels e1)-e2) depict the evolution of global average temperature increase.

of the climate damages are avoided. This is true for both climate damage specifications. For the disaster impact, the climate damages are more pronounced and economic growth is significantly dampened compared to the level impact.

Panels b1)-b2) indicate that the consumption-output ratio is in a narrow range between 74% to 77%. In particular, for the BAU case, the optimal consumption-output ratio sharply increases for high temperatures around 4°C. A potential explanation is the convexity of the climate damage function, which leads to a higher sensitivity to atmospheric temperature. For the other climate damage specification, which is linear in temperature, optimal consumption exhibit small variation across states. Under BAU optimal consumption is almost constant.

Panels c1)-c2) depict the evolution of the carbon dioxide emissions that are significantly dampened compared to under BAU. In general, the variation of optimal emissions is low. As discussed in the previous section, optimal emissions are mainly driven by the share of brown capital, while the influence of temperature is relatively weak. The small variation of the optimal carbon dioxide emissions thus follows from the small variation in S depicted in Panels d1)-d2). The evolution of the share of brown capital is crucial for understanding the interaction between the diversification and the abatement motive. If we disregard damages from climate change, the share of brown assets eventually stabilizes at $S^* = 50\%$. On the other hand, if society recognizes climate change and fights global warming, the share of brown capital decreases to approximately 20%. However, brown capital does not vanish completely since some positive amount is kept to satisfy the diversification motive. In this sense, the diversification motive eventually reduces climate action.

D.2 Effects of Climate Policy on Asset Prices

Figure A.5 complements the results presented in Figure A.4 with asset pricing results. Panels a1)-a2) depict the evolution of the green Tobin's Q, whereas Panels b1)-b2) show the evolution of the brown one. In the optimum, the green Tobin's Q decreases over time, but the brown Tobin's Q remains always smaller than the green Tobin's Q. For the disaster impact of climate change, the green Q stabilizes around 1.5, while for the level impact of climate change the green Tobin's Q continues to decrease below that level.

Panels c1)-c2) show that the equilibrium risk-free interest rate decreases for all scenarios including BAU, since over time the expected damages from global warming become more pronounced and households respond with higher precautionary savings. This effect is much

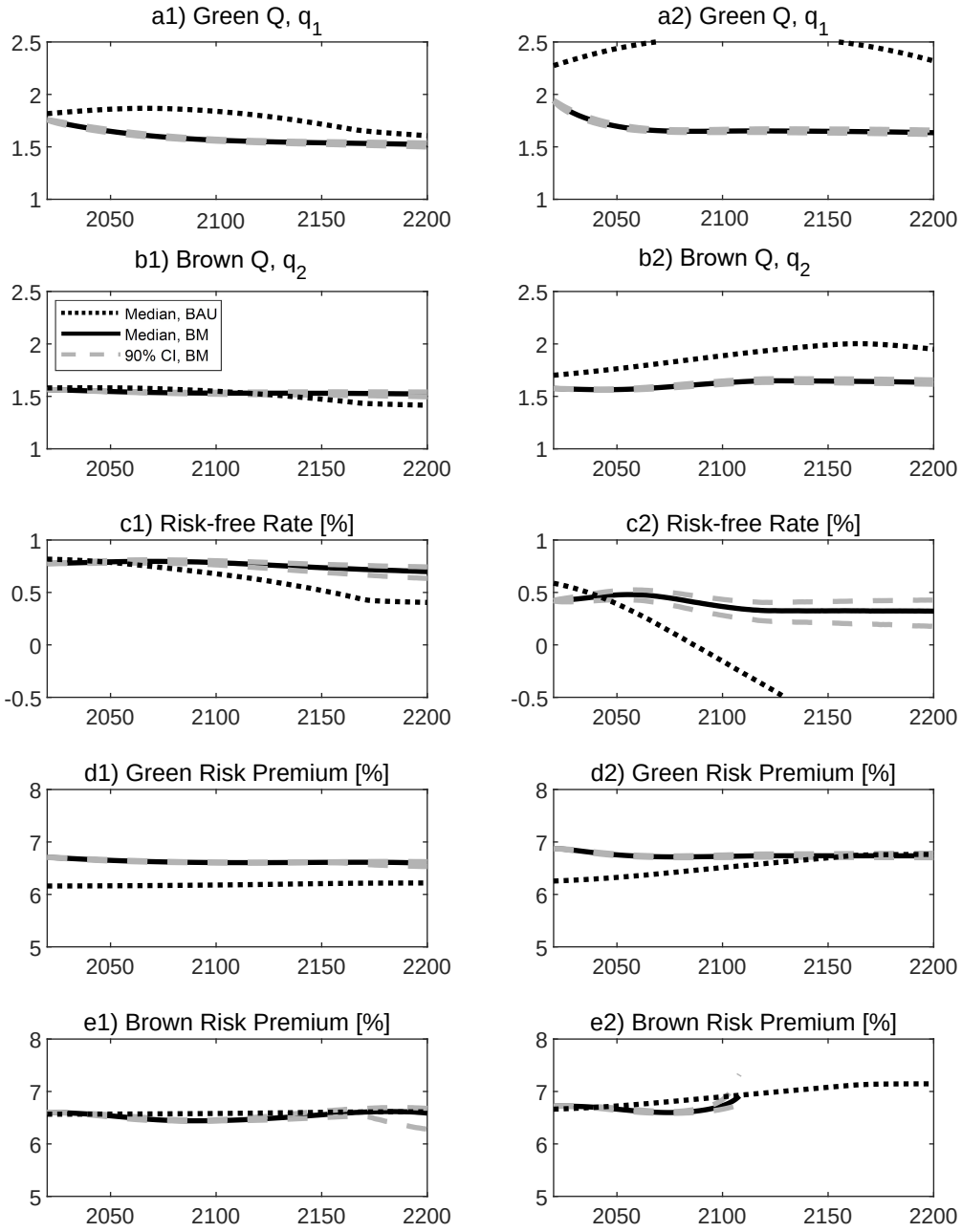

Figure A.5: Evolution of Tobin's Q's, Risk-Free Rates and the Risk Premia. The figure depicts the simulation of the asset pricing quantities for the two climate damage level impact (1st column) and disaster impact (2nd column) until the year 2200. Median optimal paths are depicted by solid lines (——) and median BAU paths by dotted lines (·····). Dashed lines (- - -) show 5% and 95% quantiles of the optimal solution. Panels a1)-a2) show the evolution of the Tobin's Q of the green asset and Panels b1)-b2) depict the evolution of the Tobin's Q of the brown asset. Panels c1)-c2) depict the evolution of the equilibrium risk-free rate. Panels d1)-d2) show the evolution of the risk premium of the green asset. Panels e1)-e2) depict the evolution of the risk premium of the brown asset.

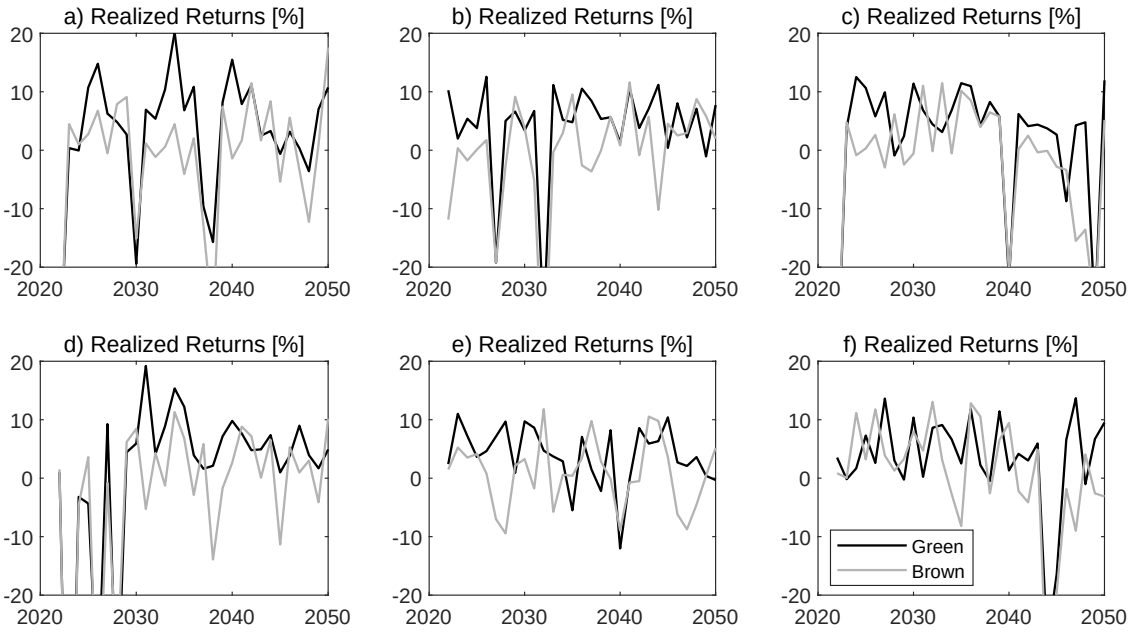

Figure A.6: Sample Paths of Green and Brown Returns. The figure depicts six sample paths of asset returns on the green and brown portfolios for a damage level impact until the year 2050. Green returns are depicted by black lines (——) and brown returns by gray lines (——). The estimated correlation between green and brown returns ranges between 20% (Panel e) and 93% (Panel d) for this 30-year time window.

stronger under BAU, since then climate damages are more severe. In contrast, if carbon is optimally priced, the downward trend of the risk-free interest rate is less pronounced.

Panels d1)-d2) show the evolution of the green risk premium, whereas Panels e1)-e2) depict the evolution of the brown risk premium. As discussed in the main text, the brown risk premium depends on the state variables S and T in a non-linear way. This might explain the "snake-shaped" evolution of the brown risk premium over time. For the disaster impact, the risk premiums are higher. This is triggered by the additional Poisson shock N_e which gives rise to an extra component in the risk premium, as seen in Proposition A.2. Since the jump intensity increases in temperature and global warming becomes more significant over time, the relative importance of the extra component increases under BAU. This reflects the fact that asset holders must be compensated for the increasing climate risks.

Finally, Figure A.6 depicts some sample paths of realized returns on green and brown assets for a level impact. The corresponding figure for climate disasters are similar and available upon request. It is shown that both assets have a strong co-movement in our scenarios. The total correlation between green and brown assets is driven by the instantaneous correlation ρ_{12} between the Brownian shocks, the common macroeconomic disasters N_e, as well as the

common risk-factors S and T, which influence dividend growth of both assets. Consequently, there is much more of a correlation than indicated by the value of ρ_{12}. Even though we assume $\rho_{12} = 0$ in our benchmark calibration, the average total correlation between green and brown assets is as high as 75% in our simulations. If we relaxed our assumptions on common disaster shocks, the total correlation between green and brown assets would decrease and the diversification motive would be even more pronounced. The corresponding figure for climate disasters are similar and available upon request. In this case, the total correlation between green and brown assets is even a bit stronger due to common climate disasters. Moreover, our model generates significantly higher realized returns for green assets than for brown assets. Green assets outperform brown assets on average by about 4.4% per year even though asset returns are highly correlated. This is qualitatively in line with the empirical findings of Pastor et al. (2022).

E Robustness

This section provides some robustness checks for our main results. We only report results for the share of brown capital and temperature but results for the optimal carbon tax, asset pricing moments, and other things are available upon request. We emphasize that these results are quite robust as well with respect to different calibrations and model specifications.

E.1 Decomposition of Climate Action with Climate Disaster Impact

We first analyze the decomposition of climate action into its three components for the model with climate disasters:

$$\text{Climate Action} = \text{Diversification } (\blacksquare) + \text{Abatement } (\blacksquare) + \text{Interaction } (\blacksquare).$$

Here, the damages are significantly more pronounced than for the level impact, and the abatement motive dominates the diversification motive as can be seen in Figure A.7. Hence, the carbon-intensive capital stock is eventually run down completely, so that the dark gray area, which represents the abatement motive, becomes bigger and the transition to a low-carbon economy takes place at a much faster pace even though the diversification motive hampers the transition to net-zero somewhat in the long-run.

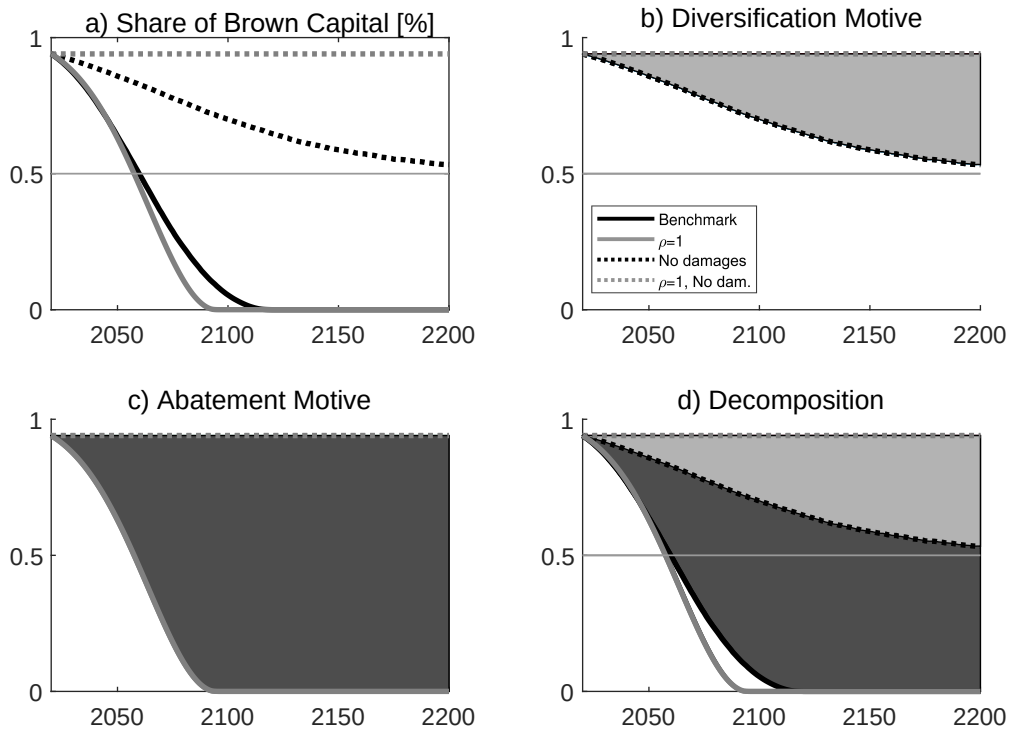

Figure A.7: Abatement and Diversification Motives with Climate Disasters. The lines depict the optimal evolution of the share of brown capital for four different calibrations until the year 2200: (i) a model without damages from climate change and perfectly correlated diffusive risk, see gray dotted lines (⋯⋯); (ii) a model without damages from climate change and zero instantaneous correlation, see black dotted lines (⋯⋯); (iii) a model with the disaster damage specification and perfectly correlated diffusive risk, see gray lines (——); (iv) the benchmark model with the disaster damage specification and uncorrelated diffusive risk. The areas in b), c), and d) depict the strenghts of the diversification motive (■), the strength of the abatement motive (■), and the interaction of diversification and abatement motives (■), in scenarios (ii), (iii), and (iv), respectively.

E.2 Unleveraged Dividends

We now study an alternative calibration with non-leveraged dividends, i.e., we set $\varphi = 1$. This implies that dividends are equally volatile as consumption and dividends fall as much as consumption when a disaster hits the economy. This approach requires a higher relative risk aversion of $\gamma = 5.368$ to match the equity premium of 6.6%. To match the other figures as well, we need in particular a high time preference rate of $\delta = 5.09\%$. Those preference parameters are in line with Pindyck and Wang (2013) and the market-based calibration in van den Bremer and van der Ploeg (2021). In turn, we discount at a higher rate, which also leads to much smaller optimal carbon prices. Therefore, the transition towards a low-carbon economy takes place at a slower pace and the benefits from abatement and diversification

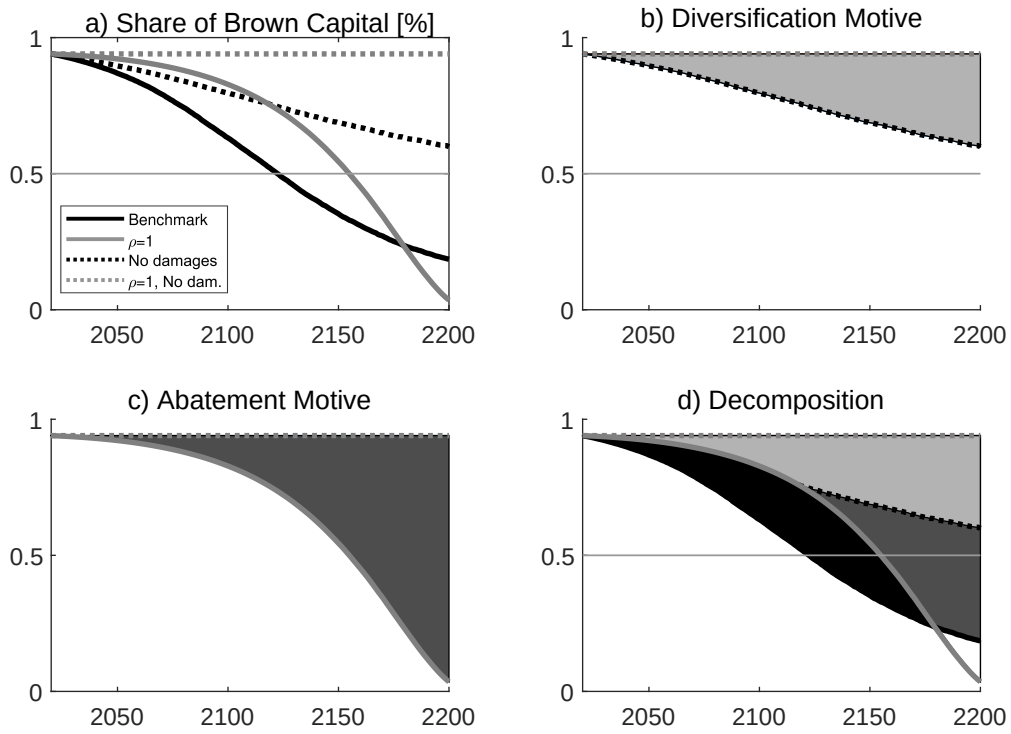

Figure A.8: Abatement and Diversification Motives with Unleveraged Dividends. The lines depict the optimal evolution of the share of brown capital for four different calibrations until the year 2200: (i) a model without damages from climate change and perfectly correlated diffusive risk, see gray dotted lines (⋯⋯); (ii) a model without damages from climate change and zero instantaneous correlation, see black dotted lines (⋯⋯); (iii) a model with the Nordhaus damage specification and perfectly correlated diffusive risk, see gray lines (——); (iv) the model with the Nordhaus damage specification and uncorrelated diffusive risk. The areas in b), c), and d) depict the strenghts of the diversification motive (■), the strength of the abatement motive (■), and the interaction of diversification and abatement motives (■), in scenarios (ii), (iii), and (iv), respectively.

are less pronounced as can be seen in Figure A.8. However, our results are qualitatively robust to this alternative calibration.

E.3 Learning by Doing: Social Cost of Carbon

Figure A.9 shows the median optimal carbon price (——) and its 5% and 95% quantiles and compares it to the optimal carbon price in the benchmark specification without learning by doing (⋯⋯). It can be seen that with learning by doing the optimal carbon price is a bit lower as the transition towards a low-carbon economy is slightly accelerated by the LBD motive. This is well in line with Panel c) of Figure 5, where the abatement motive is less pronounced than in the benchmark case.

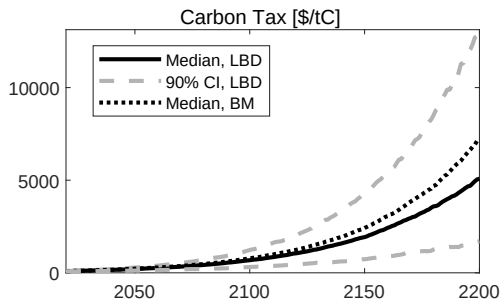

Figure A.9: Time Paths for the Optimal Carbon Taxes. The figure depicts the time paths of the optimal carbon taxes Median optimal paths are depicted by black solid lines (——). Dashed lines (- - -) show 5% and 95% quantiles of the optimal time paths. The median time path for the carbon taxes in the benchmark model without LBD are depicted by dotted lines (·····).

E.4 Learning by Doing: Alternative Specification

Here we analyze how the LBD motive (see Section 6.3) interacts with the diversification and abatement motive if we calibrate the declining cost of green energy to be in line with the historical price development of solar modules.[39] Extrapolating this trend, we expect that prices for green energy will at some point fall below prices for fossil fuel making the green sector more efficient compared to the brown sector. Figure A.10 depicts the results. It can be seen from the figure that the LBT motive already leads to a very quick transition towards a low-carbon economy (·····). When the effect from diversification kicks in, the transition is accelerated even more at the beginning, but is slowed down as you move away from the optimum. These results are well in line with our previous findings but now the LBD motive is the dominant driver for the transition towards net-zero.

E.5 Heterogeneous Volatilities

Consider the effects of different capital volatilities. We fix the capital volatility of the green sector at $\sigma_1 = 0.02$ and vary the volatility of the brown sector, $\sigma_2 \in \{0.02/\sqrt{2}, 0.02, 0.02\sqrt{2}\}$ (corresponding to "low risk", benchmark, and "high risk"). Figure A.11 depicts the results. If we disregard the effects of climate change, the optimal long-term shares of the brown sector are 2/3, 1/2, and 1/3 (dotted lines). An interesting effect arises if we take climate change into account. As can be seen from the results for the Nordhaus calibration in Panel a1), the relative reduction of the brown sector resulting from climate damages is strongest if

[39] We still assume a cost function of the form $b_1 = k_0(1-S)^{-k_1}$ and assume that costs for renewable energy drop by 30% for every doubling of cumulative installed volume. This leads to $k_0 = 0.2351$ and $k_1 = 0.5146$, see Swanson's law.

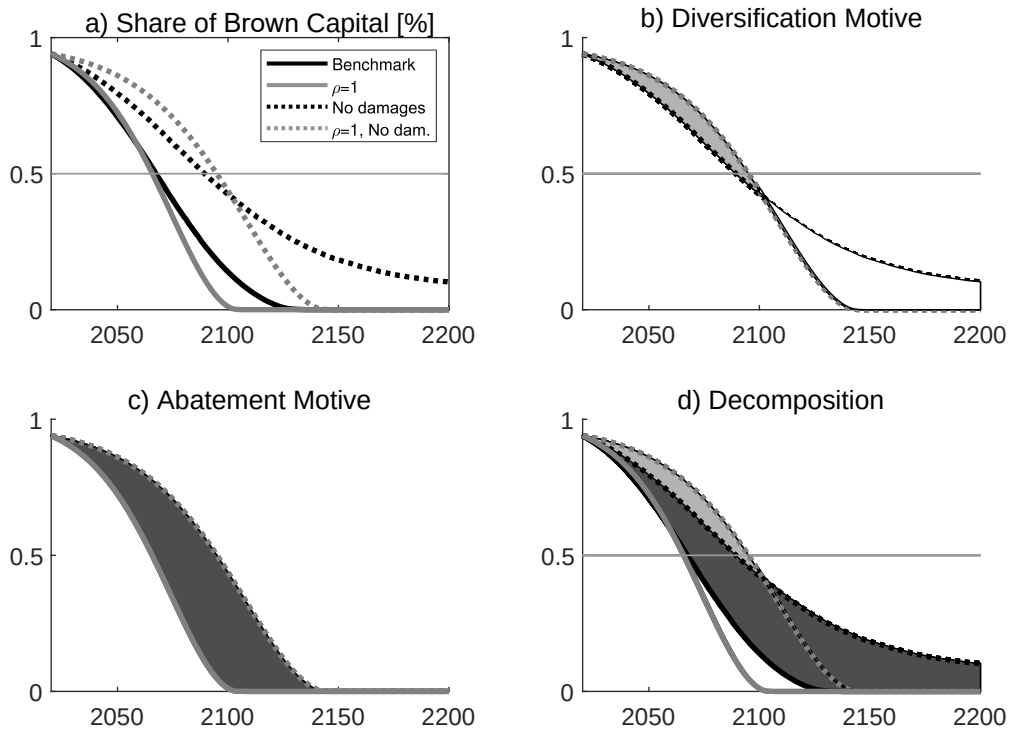

Figure A.10: Abatement and Diversification Motives with Accelerated Green Transition Driven by Directed Technological Change: Faster Cost Reductions Based on Solar Power Experience. The lines depict the optimal evolution of the share of brown capital for four different calibrations until the year 2200: (i) a model without damages from climate change and perfectly correlated diffusive risk, see gray dotted lines (·····); (ii) a model without damages from climate change and zero instantaneous correlation, see black dotted lines (·····); (iii) a model with the Nordhaus damage specification and perfectly correlated diffusive risk, see gray lines (——); (iv) the model with the Nordhaus damage specification and uncorrelated diffusive risk. The areas in b), c), and d) depict the strenghts of the diversification motive (■), the strength of the abatement motive (■), and the interaction of diversification and abatement motives (■), in scenarios (ii), (iii), and (iv), respectively.

the volatility of the brown sector is small, i.e., if the brown sector has a high diversification potential ("low risk") without damages from climate change (····· vs. ——). In this case, the optimal share of the brown sector drops from 66% to 26%. In the benchmark case, this share is 20% instead of 50%. In the high-risk scenario, the optimal share of the brown sector drops from 33% to 15%.

The reason for the more pronounced climate action in the low-risk environment becomes clear if we look at Panel a2) depicting the temperature paths. If there is no effect of climate change on capital (·····), the temperature is highest in the low-risk scenario. Therefore, the planner reacts most if damages are internalized (——). Consequently, the total effect of the abatement motive is biggest in the low-risk scenario even though the share of brown

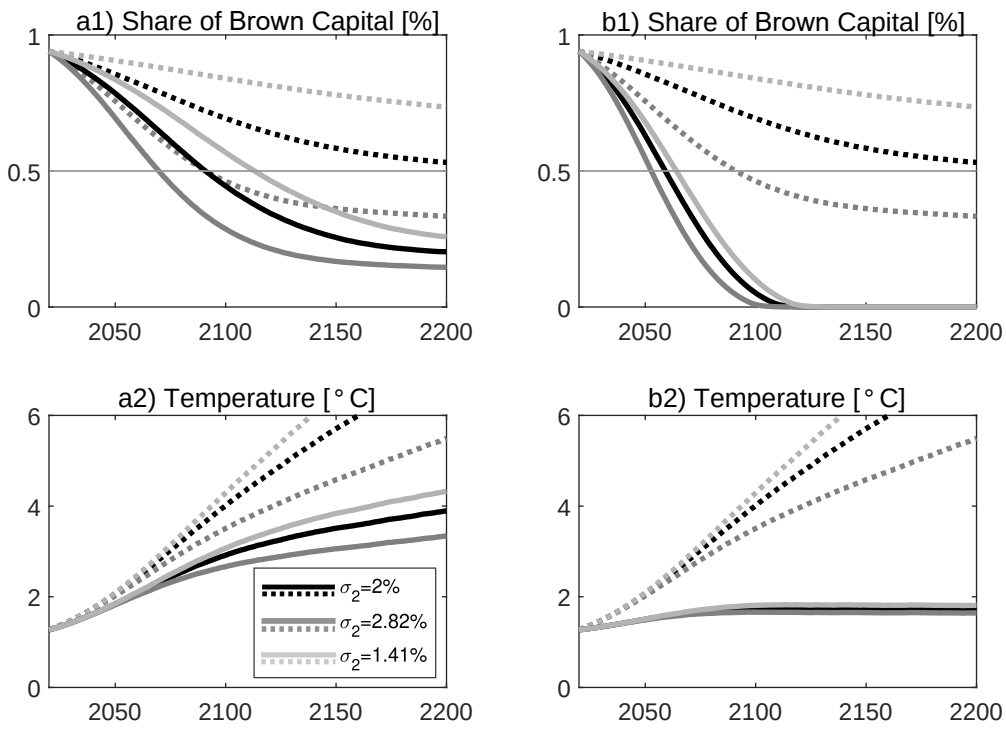

Figure A.11: Heterogeneous Volatilities. Solid lines depict the optimal evolution of the share of brown capital and global average temperature for the two climate damage specifications, i.e., level impact (1st column) and disaster impact (2nd column), until the year 2200. Dotted lines show the results for hypothetical scenarios without damages from climate change. Black lines (⋯⋯, ——) show results for the benchmark case where the volatilities are identical. Gray lines (⋯⋯, ——) show results for a higher volatility of shocks to the brown sector, $\sigma_2 = 0.02\sqrt{2} = 0.0282$. Light lines (⋯⋯, ——) depict the results for a lower volatility of shocks to the brown sector, $\sigma_2 = 0.02/\sqrt{2} = 0.0141$.

capital and temperature are higher than in the benchmark case (⋯⋯, ——). Our findings are confirmed by Panels b1) and b2) that show the reductions for a disaster impact from climate change. The abatement motive is more pronounced for a disaster impact since the economic consequences for this damage specification are much more severe than for a level impact.

E.6 Higher and Lower Instantaneous Volatilities

This section complements Section E.5, which studies the influence of asymmetric instantaneous volatilities. Now, we study the effect of symmetric volatilities that differ from our benchmark calibration. Figure A.12 depicts the results. The black lines (⋯⋯, ——) show the results for the benchmark case with $\sigma_n = 2\%$. The light lines (⋯⋯, ——) depict the results for higher volatility, $\sigma_n = 3\%$, and the gray lines (⋯⋯, ——) show the results for lower volatility, $\sigma_n = 1\%$. The figure shows that lower volatility decreases the importance of the diversifi-

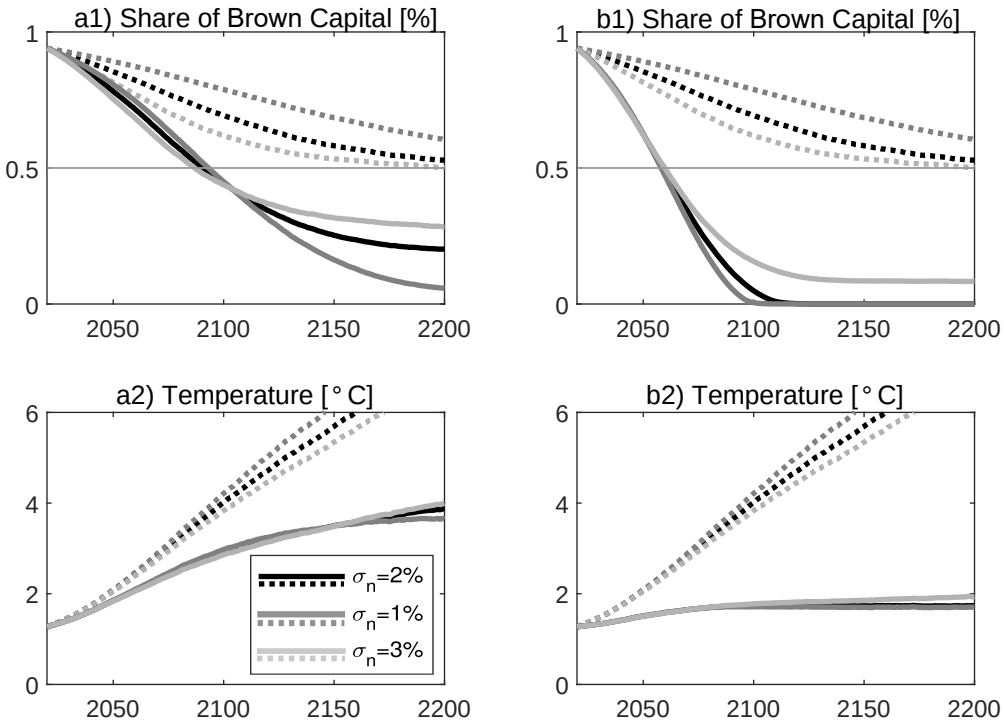

Figure A.12: Higher and Lower Different Instantaneous Volatilities. Solid lines depict the optimal evolution of the share of brown capital and global average temperature for the two climate damage specifications, i.e., level impact (1st column) and disaster impact (2nd column), until the year 2200. Dotted lines show the results for hypothetical scenarios without damages from climate change. Black lines (⋯⋯,——) show results for the benchmark case where $\sigma_n = 2\%$. Gray lines (⋯⋯, ——) show results for a lower volatility of shocks to the brown sector, $\sigma_n = 1\%$. Light lines (⋯⋯, ——) depict the results for a higher volatility of shocks to the brown sector, $\sigma_n = 3\%$.

cation motive and thus society keeps less carbon-intensive capital in the economy. In the limiting case of $\sigma_n = 0$ both capital stocks would be perfectly correlated to each other, and thus the carbon-intensive capital stock would eventually be run down.

E.7 Positive and Negative Instantaneous Correlations

Correlations play a crucial role for diversification. Figure A.13 depicts the optimal evolution of the share of brown capital for different values of the instantaneous correlation ρ_{12} and for the two climate damage specifications, level impact (1st column) and disaster impact (2nd column). Black lines (⋯⋯,——) show results for the benchmark case $\rho_{12} = 0$. Gray lines (⋯⋯, ——) show results for $\rho_{12} = -0.5$. Light lines (⋯⋯, ——) depict results for $\rho_{12} = 0.5$. Dotted lines depict results for hypothetical scenarios without damages from climate change.

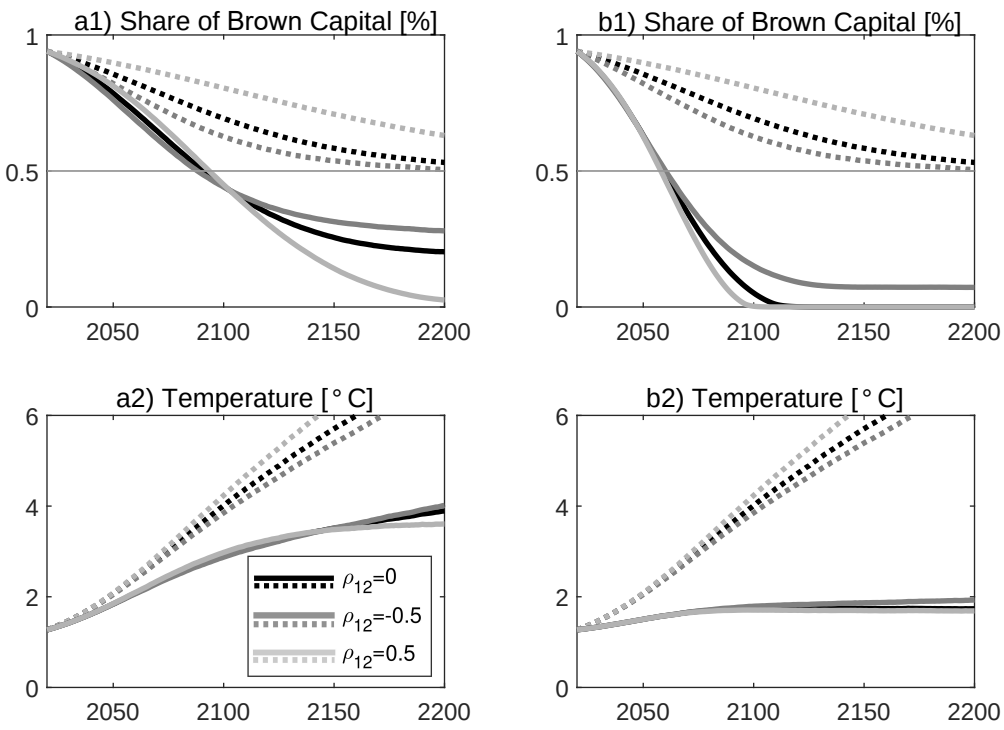

Figure A.13: Positive and Negative Different Instantaneous Correlations. Solid lines depict the optimal evolution of the share of brown capital and global average temperature for the two climate damage specifications, i.e., level impact (1st column) and disaster impact (2nd column), until the year 2200. Black lines (⋯⋯,——) show results for the benchmark case where the correlation between the Brownian shocks affecting the green and brown sector is $\rho_{12} = 0$. Gray lines (⋯⋯, ——) show results with $\rho_{12} = -0.5$. Light lines (⋯⋯, ——) depict the results with $\rho_{12} = 0.5$. Dotted lines show the corresponding results for hypothetical scenarios without damages from climate change.

A negative correlation coefficient (⋯⋯, ——) amplifies the diversification motive. This leads to a faster transition to full diversification of $S = 50\%$. In the short run, this effect accelerates decarbonization of the economy, but in the long run the opposite is true, see Panels a1)-a2) of Figure A.13. The economy keeps a higher share of brown capital to benefit from diversification even in case of the disaster impact. In turn, the transition is slowed down and the share of brown capital stabilizes at a higher level compared to the case with zero correlation. In other words, there is less climate action in the long run if the benefits from diversification are more pronounced.

For a positive correlation coefficient, the diversification motive is less important, which can be seen from the gray dotted lines (⋯⋯). In the short run, transition from a carbon-intensive to a carbon-free economy is significantly slowed down. In the long run, however, the abatement motive dominates and the share of brown assets stabilizes at lower levels (——). Hence,

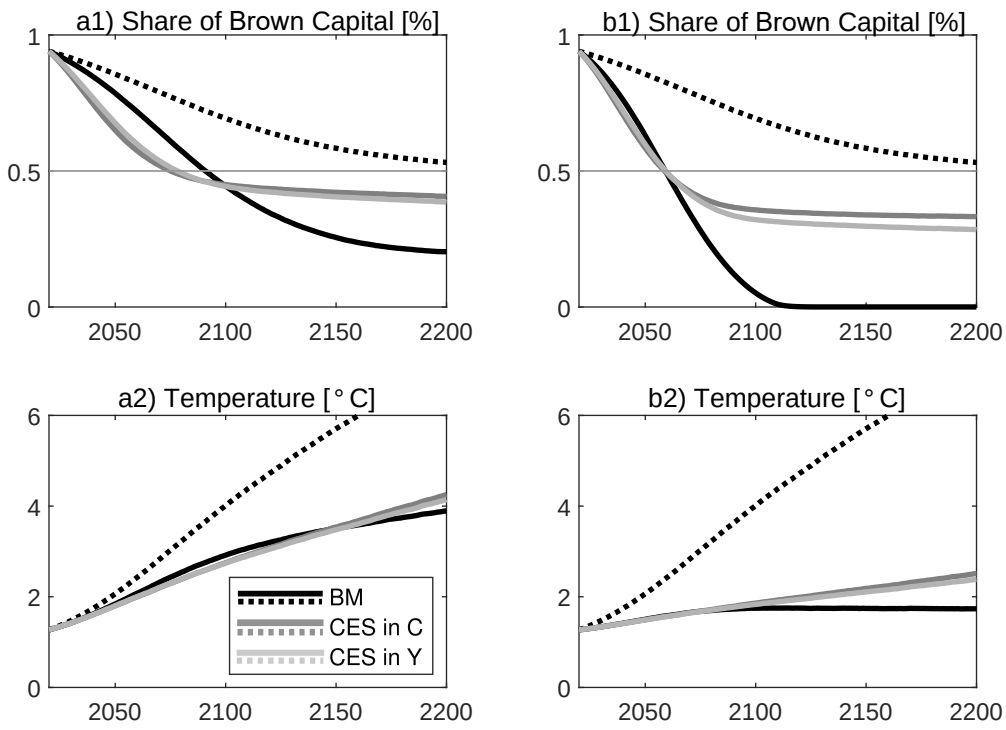

Figure A.14: Imperfectly Substitutable Final Goods. The figure depicts the simulation of the share of brown capital and global average temperature for the two climate damage specifications, i.e., level impact (1st column) and disaster impact (2nd column), until the year 2200. The black dotted lines (·····) show the results for a hypothetical scenario without damages from climate change. The black solid lines (——) show the results for benchmark setting with perfect substitutes. The gray lines (——) show results for imperfect substitutes in consumption ($\rho = 0.9$). The light lines (——) show results for imperfect substitutes in production ($\rho = 0.9$).

the speed of decarbonization is significantly effected by the sign and size of the correlation coefficient between the green and brown capital stock.

E.8 Imperfect Substitutable Final Goods

We now consider two alternative model extensions that relax the assumption of perfectly substitutable final goods. First, we assume that the consumption goods produced in both sectors are imperfect substitutes and the representative agent gains utility from a CES consumption bundle $C = \left(C_1^\rho + C_2^\rho\right)^{\frac{1}{\rho}}$, where ρ is a constant and $\zeta = \frac{1}{1-\rho}$ is the elasticity of substitution. Second, we study an extension in the spirit of Acemoglu et al. (2012) and assume that Y_1 and Y_2 are intermediate goods that must be aggregated to a final good via $Y = \left(Y_1^\rho + Y_2^\rho\right)^{\frac{1}{\rho}}$. Both extensions lead to significantly more involved first-order conditions and the solution requires additional computational costs.

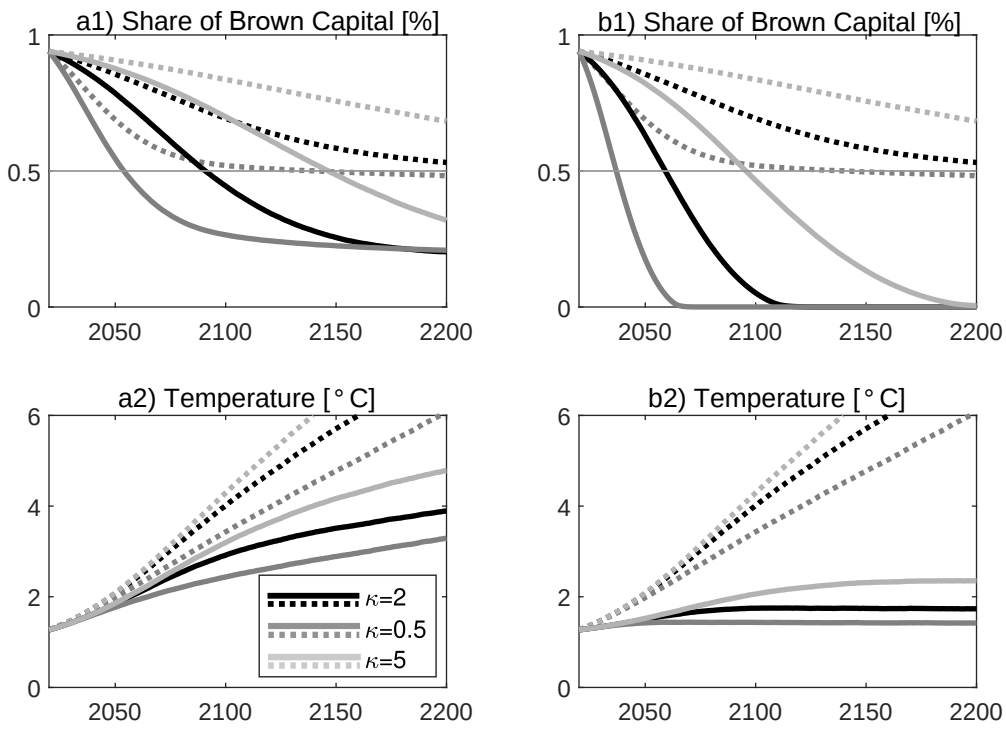

Figure A.15: Changes in the Reallocation Cost Parameter. The figure depicts the simulation of the share of brown capital and global average temperature for the two climate damage specifications, i.e., level impact (1st column) and disaster impact (2nd column), until the year 2200. The dotted lines (⋯⋯) show the results for a hypothetical scenario without damages from climate change. The black solid lines (——) show the results for a benchmark cost parameter of $\kappa = 2$. The gray lines (——) show results with a low reallocation cost parameter $\kappa = 0.5$. The light lines (——) show results for when reallocation is more expensive $\kappa = 5$.

Figure A.14 depicts the results for both model extensions each with $\rho = 0.9$ corresponding to an elasticity of substitution between the two sectors of $\zeta = 10$. The light lines (⋯⋯, ——) depict the results for imperfect substitutes in consumption, while the gray lines (⋯⋯, ——) in Figure A.14 show the results for imperfect substitutes in production. The black lines (⋯⋯, ——) show the results for the benchmark case with perfect substitutes.

In line with Acemoglu et al. (2012), we find that a higher elasticity of substitution leads to more and faster abatement. A lower elasticity between the two sectors significantly increases the demand for brown goods in order to sustain production. So, additionally to the abatement motive and the financial diversification motive, a third effect materializes, which is due to the desire to either diversify the production process or to diversify the consumption bundle. Either way, this effect hampers the transition towards a low-carbon economy.

E.9 Changes in the Reallocation Cost Parameter

Here we analyze the effect of the reallocation cost parameter κ on the interplay between diversification and climate action. Figure A.14 depicts the results. The light lines (·····, ——) depict the results for high reallocation costs, $\kappa = 5$, the gray lines (·····, ——) show the results for a low reallocation cost parameter, $\kappa = 0.5$. The black lines (·····, ——) show the results for the benchmark case with $\kappa = 2$. A higher value of the reallocation cost parameter κ leads to more sticky investment decisions as the reallocation of brown capital into green capital is more expensive. Figure A.15 shows that in the long run the optimal share of brown capital in the economy is independent of this parameter indicating that κ only influences the speed of the transition, but not the level of stabilization.

E.10 Lower Total Factor Productivity for the Green Sector

Here we analyze the effect of an asymmetric calibration of the effective total factor productivity. In the benchmark calibration both sectors are assumed to be equally productive with $A_1^* = A_2^* = 0.0449$. Now we assume that the different energy costs across the two sectors lead to different effective productivities and, in turn, the green sector generates slightly lower economic growth rates compared to the benchmark case. The black lines (·····, ——) in Figure A.16 show the results for the benchmark case. The gray lines (·····, ——) show the results for when the effective productivity of the green sector is about 1.5% smaller than the brown sector. The light lines (·····, ——) depict the results for when the effective productivity of the green sector is about 3% smaller than the brown sector. It turns out that lowering the productivity of the green sector in response to higher energy costs hampers the transition towards a low-carbon economy and the planner wants to keep a larger share of brown capital alive. Hence, as for asymmetric volatility parameters, the share of brown capital stabilizes at a level different from 50%.

E.11 Effects of Specifications with Higher Climate Damages

Figure A.17 depicts the influence of the climate damage specification on the optimal evolution of the share of brown capital and global temperature. The black dotted lines (·····) show the results for a hypothetical scenario where climate change does not generate economic damages, in which case only the diversification motive matters. If economic damages from climate change are pronounced, the abatement motive comes into play and the optimal

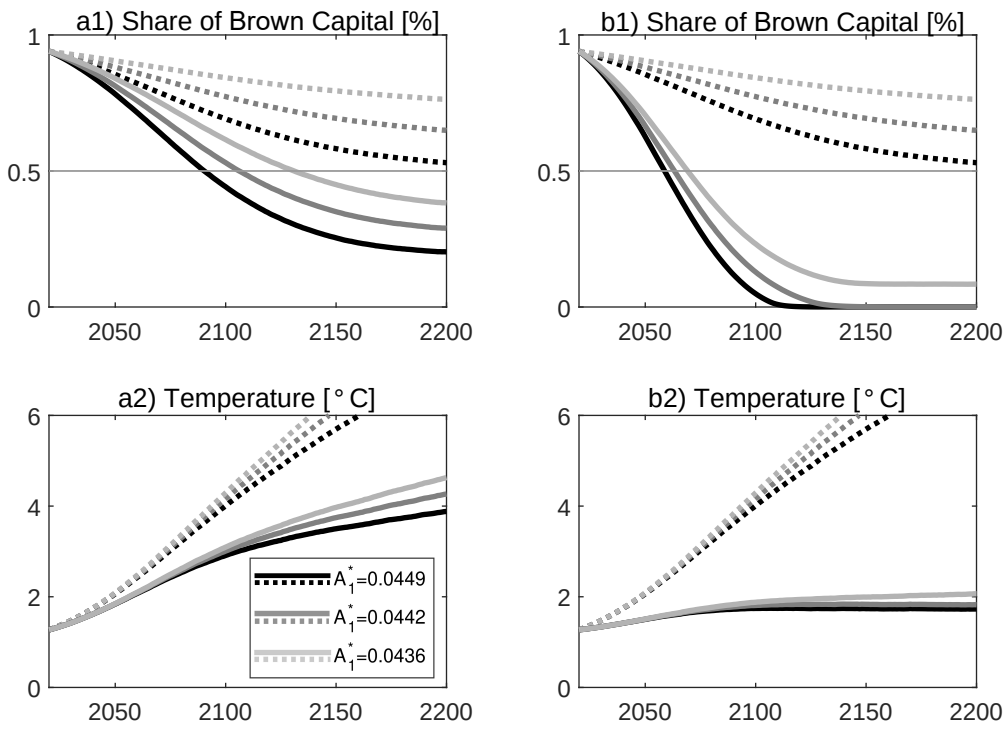

Figure A.16: Lower Total Factor Productivity for the Green Sector. The figure depicts the simulation of the share of brown capital and global average temperature for the two climate damage specifications, i.e., level impact (1st column) and disaster impact (2nd column), until the year 2200. The black dotted lines (·····) show the results for a hypothetical scenario without damages from climate change. The black solid lines (——) show the results for the benchmark values of total factor productivity $A_1 = 0.1058$, $A_2 = 0.1030$, or equivalently $A_1^* = A_2^* = 0.0449$. The gray lines (——) show results with a lower productivity of the green sector of $A_1 = 0.1044$, or equivalently $A_1^* = 0.0442$, i.e., about 1.5% smaller than the carbon-intensive sector. The light lines (——) show results for when $A_1 = 0.1030$, or equivalently $A_1^* = 0.0436$, i.e., about 3% smaller than the carbon-intensive sector.

level of the share of brown capital shifts down to a social optimum below $S = 50\%$. The black solid lines (——) show the results for the climate damage parameters presented in Section 5. The gray lines (——) depict results with damage parameters that are twice as high. The light lines (——) show results with damage parameters that are three times higher. Table A.2 summarizes the climate damage parameters that are used in Figure A.17. It can be seen that for higher damage parameters the abatement motive becomes more pronounced and the diversification motive loses its importance. For sufficiently high climate damages, the brown capital stock vanishes and production of brown goods ceases. This increases the volatility of total capital, but the benefits from abatement eventually dominate the benefits from diversification. Doubling or tripling the climate damage parameter for the disaster impact has only a moderate influence since the benchmark calibration is already severe

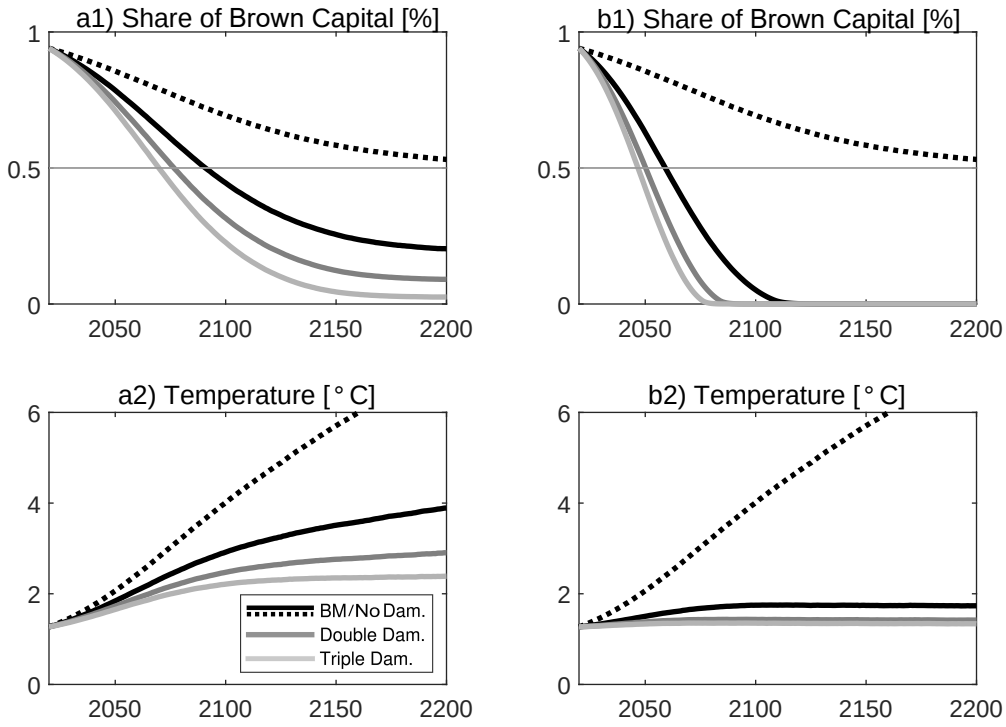

Figure A.17: Increasing Intensities of Global Warming Damages. The figure depicts the simulation of the share of brown capital and global average temperature for the two climate damage specifications, i.e. level impact (1st column) and disaster impact (2nd column), until the year 2200. The black dotted lines (·····) show the results for a hypothetical scenario without damages from climate change. The black solid lines (——) show the results for the damage parameters as calibrated in Section 5. The gray lines (——) show results with damage parameters that are twice as high as in the benchmark calibration. The light lines (——) show results with damage parameters that are three times higher than those from the benchmark calibration. The main insight from this figure is that with higher intensities of damages than our benchmark damages, the abatement motives becomes relatively more important than the diversification motive and leads to a lower or even a zero brown capital stock in the long run.

enough to bring the share of brown capital to zero. The effect for the level impact of climate change is more pronounced.

Figure A.18 shows the effects of a *simultaneous* level and disaster impact of climate change (——). Since the disaster impact (——) is much more pronounced than Nordhaus' level impact (——), the latter is dominated by the disaster impact. Hence, switching on the level impact does not lead to significantly more abatement, nor signifacantly higher carbon taxes (not shown in the figure).

Impact	Benchmark (——)	Double Impact (——)	Triple Impact (——)
Level	$\theta_i = 0.00236$	$\theta_i = 0.00472$	$\theta_i = 0.00708$
Disaster	$\lambda_c(T) = 0.003 + 0.096T$	$\lambda_c(T) = 0.003 + 0.192T$	$\lambda_c(T) = 0.003 + 0.288T$

Table A.2: Different Intensities for the Specifications of Global Warming Damages. The table summarizes the different climate damage specifications that are used in Figure A.17.

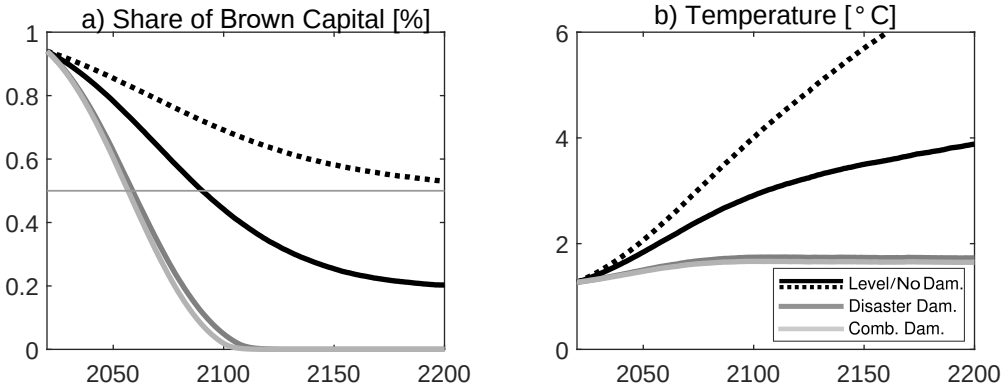

Figure A.18: Combining Different Types of Climate Damage Specifications. The figure depicts the simulation of the share of brown capital and global average temperature for the damage specifications level impact (——), disaster impact (——), and combined level and disaster impact (——) until the year 2200. The black dotted lines (·····) show the results for a hypothetical scenario without damages from climate change.

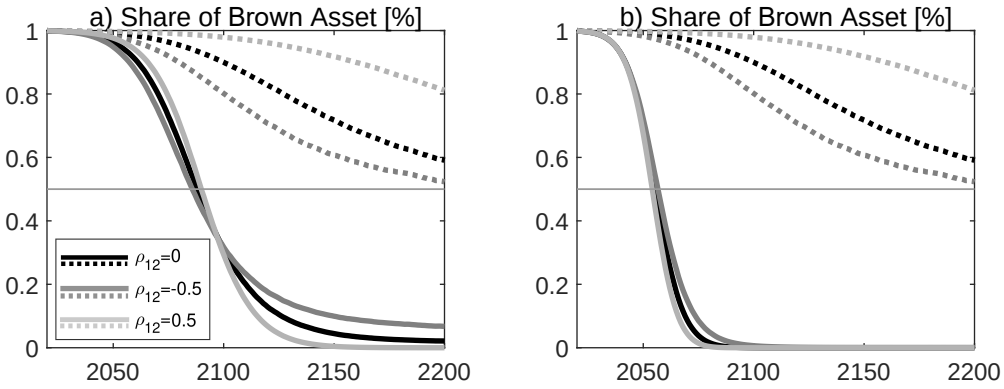

Figure A.19: Brown Portfolio Shares for Different Instantaneous Correlations. Solid lines depict the optimal evolution of the share of the brown asset $\pi = P_2/(P_1 + P_2)$ for the two climate damage specifications, i.e., level impact (1st column) and disaster impact (2nd column), until the year 2200. Black lines (·····,——) show results for the benchmark case where the correlation between the Brownian shocks affecting the green and brown sector is $\rho_{12} = 0$. Gray lines (·····, ——) show results with $\rho_{12} = -0.5$. Light lines (·····, ——) depict the results with $\rho_{12} = 0.5$. Dotted lines show the corresponding results for hypothetical scenarios without damages from climate change.

E.12 Effects on Brown Portfolio Share

While S denotes the share of brown capital, we are also interested in the share π of brown assets in the world portfolio held by the representative investor, i.e.,

$$\pi = \frac{P_2}{P_1 + P_2}. \tag{E.1}$$

Figure A.19 depicts the analogous results for the share of brown assets instead of the share of brown capital. We find that the results are qualitatively similar although the asset shares stabilize at lower levels than the capital shares. This can be explained by the fact that the green asset has lower dividend yields than the brown asset, hence the green asset prices grow faster than the brown asset prices (see Table 2) and the denominator in (E.1) eventually becomes relatively larger than the denominator in the definition of S.